



Study on Microwave Assisted Synthesis of Biodegradable Guar Gum Grafted Acrylic Acid Superabsorbent Nanocomposites

S. Menon¹, M.V. Deepthi², R.R.N. Sailaja^{2*}, G.S. Ananthapadmanabha³

¹National Institute of Technology Karnataka (NITK), Surathkal-575 025

²The Energy and Resources Institute (TERI), Southern Regional Centre, Bangalore-560 071

³Sri Jayachamarajendra College of Engineering (SJCE), Mysore-570 006

Received 1st April 2014; Accepted 21st April 2014.

Editor in Chief: Dr. K.S.V. Krishna Rao; Guest Editors: Dr. Siddaramaiah, Dr. G. M. Shashidhara.

Presented at the POLYCON-2014, 6th National Conferences on Advances in Polymeric Materials [Energy, Environment & Health] (NCAPM), Mysore, India, 25-26 April 2014.

ABSTRACT

Polysaccharide based semisynthetic polymers are gaining prominence as eco-friendly alternatives in many fields. Thus in this study, guar gum grafted poly acrylic acid/cloisite superabsorbent nanocomposites were prepared by both conventional and microwave methods. The reaction parameters such as initiator concentration, monomer concentration and time were optimized and the effect of cross-linker and cloisite concentration on swelling were also studied. Characterization of the synthesized polymer was carried out using FTIR, XRD, DSC and TGA. The final optimized percentage grafting in conventional and microwave methods were observed to be 60% and 63% respectively. The microwave method was twelve times faster than the conventional method. The swelling and reswelling studies of the composites were conducted the biodegradability of the composites were also studied.

Keywords: Polysaccharide superabsorbent, microwave grafting, guar gum, nanocomposites, swelling.

1. INTRODUCTION

Superabsorbents are hydrophilic polymer networks which can absorb and retain large amounts of aqueous fluids [1]. Superabsorbents have found extensive applications in many fields such as agriculture [2], hygienic products [3], wastewater treatment [4] and drug delivery systems [5], etc. Conventionally Superabsorbents are completely petroleum based polymers, which are not only expensive but also are not environmentally friendly. Due to increasing environmental concern, polysaccharide based materials have gained importance [6]. The natural abundance and universal presence as a renewable resource makes polysaccharides even more desirable. Even though polysaccharides (such as guar gum), have natural resistance to degradation under shear, they have poor shelf life because of their susceptibility to biodegradation. Synthetic polymers on the other hand can be easily tailored but they have poor shear resistance properties. Chemical grafting helps combine the beneficial properties of both and create graft polymers [7], which are environmentally friendly and whose properties can be engineered suitably. The generally used conventional grafting method involves producing

free radical sites in situ on polysaccharide backbones using chemical initiators such as ceric ammonium nitrate, ammonium/potassium persulfate. The major drawback of the conventional method is that they require inert working conditions and are very time consuming. Moreover the copolymer products are often accompanied by homo-polymer formations which besides decreasing the yield, apart from contaminating the co-polymeric product. They also may lead to polysaccharide backbone degradation [7]. Unlike conventional grafting reactions, microwave assisted synthesis enhances copolymer formation and thus results in better copolymer yield in short reaction times. The provision of electronic control of microwave power and time of irradiation helps control the percentage of grafting. Composites of polymers with clay minerals reduce production cost and improve the performance of the material [8]. They are easily available and are used widely to improve the property of biomaterials [9]. Generally modified clay minerals are used owing to their greater dispersability in the polymeric matrix. [10]. Clays in their natural form are not suitable for mixing and interacting with most polymer matrices. Therefore, they must be treated to improve its

*Corresponding Author:

Email: rrnsb19@rediffmail.com

Phone: +91 080-25356590

dispersability. Commonly used treatment methods nowadays are surface modification, ion exchange and organically modified clay such as Cloisite [11]. In this study, guar gum-grafted-Poly acrylic acid/cloisite superabsorbent nanocomposites have been synthesized with the aim of developing new kinds of superabsorbent composites with improved structure, properties and environmentally friendly characteristics. The conventional and microwave methods are compared and parameters are optimized for better yield. The grafted product has been characterized and swelling and biodegradability characteristics have also been studied.

2. EXPERIMENTAL

2.1 Materials

Guar gum, Acrylic acid (for synthesis), Ammonium persulfate (APS), N,N'-methylene-bis-acrylamide (MBA, analytical grade) were obtained from Sd Fine Chemicals, India. Organically modified clay (Cloisite 30B) was purchased from J.K. Impex, India.

2.2 Preparation of GG-g-PAA in conventional method

1% (w/v) guar gum solution was prepared in distilled water in a beaker and was stirred. Acrylic acid was added to this solution (6% solution v/v) and mixed steadily till the temperature was 60°C. APS (0.095% w/v) was added as an initiator and 0.095% w/v of MBA was added as a crosslinking agent. After a reaction period of 60 mins, the reaction mixture was allowed to cool to room temperature and was neutralized with 1N NaOH solution. The resultant mixture was precipitated using acetone. It was repeatedly washed with acetone to remove the homopolymer and unreacted monomer. The precipitated sample was strained and dried in a hot air oven for 5-6 hours at 60°C. The dried sample was weighed and the graft percentage and graft efficiency were calculated using the following equations.

$$\text{Grafting Percentage} = \frac{W_1 - W_0}{W_0} \times 100 \quad (1)$$

$$\text{Grafting Efficiency} = \frac{W_1 - W_0}{W_2} \times 100 \quad (2)$$

Where, W_0 = Weight of Guar gum (g), W_1 = Weight of GG-g-PAA (g), W_2 = Weight of monomer used in the reaction (g)

2.3 Preparation of GG-g-PAA in microwave method

The solution was kept in a microwave system with provision for stirring. The reaction was carried out as mentioned above with initiator concentration 0.095% w/v, Monomer concentration 0.095% w/v and Acrylic Acid concentration 6.5 % v/v. The

reaction time was 4.5 minutes. The product was obtained as above. The graft percentage and graft efficiency were calculated using equations (1) and (2).

2.4 Fourier transforms infrared spectroscopy analysis (FTIR)

FTIR analysis of GG-g-PAA and GG-g-PAA/cloisite were performed using Perkin-Elmer spectrum 1000 FTIR instrument.

2.5 X-ray diffraction studies (XRD)

XRD measurements for the composites have been performed using a sing advanced diffractometer [PANalytical, XPERT-PRO] equipped with Cu K α radiation source ($\lambda = 0.154$ nm). The diffraction data were collected in the range of $2\theta = 3-20^\circ$.

2.6 Swelling studies

Swelling in different pH buffers and salt concentrations, A series of GG-g-PAA/Cloisite samples were prepared with varying Cloisite concentrations (between 0-10% w/w). For each set, muslin tea bags containing known weight of samples were prepared and immersed in Acidic buffer of pH 4 and allowed to soak for an hour. After an hour they were removed and hung up for 15 minutes to remove the excess buffer and weighed. The equilibrated swelling (ES) was found out using the following equation.

$$ES = \frac{W_2 - W_1}{W_2} \quad (3)$$

Where, W_1 = Weight of dry sample (g), W_2 = Weight of Swollen gel (g), This procedure was done in triplicates and was repeated for neutral and basic buffers also. The swelling capacities of the superabsorbent nanocomposites were determined in 5, 10, 20, 50 and 100 mM NaCl respectively.

2.7 Thermo Gravimetric Analysis

The Thermo Gravimetric Analysis (TGA) of the composites was carried out using the Perkin-Elmer Pyris Diamond 6000 analyser in an atmosphere of nitrogen. The samples were subjected to heating in a range of 20° - 800°C at a rate of 10°C/min.

2.8 Differential Scanning Calorimetry

DSC of the composites was performed using a Mettler Toledo model DSC 822e instrument (Mettler Toledo AG). Samples were placed in sealed aluminum cells with a quantity of less than 10 mg and scanning at a heating rate of 10°C/min in a heating range of 0°C to 350°C

2.9 Biodegradability studies

The biodegradability of the samples was tested in natural soil. The samples were dried and buried in

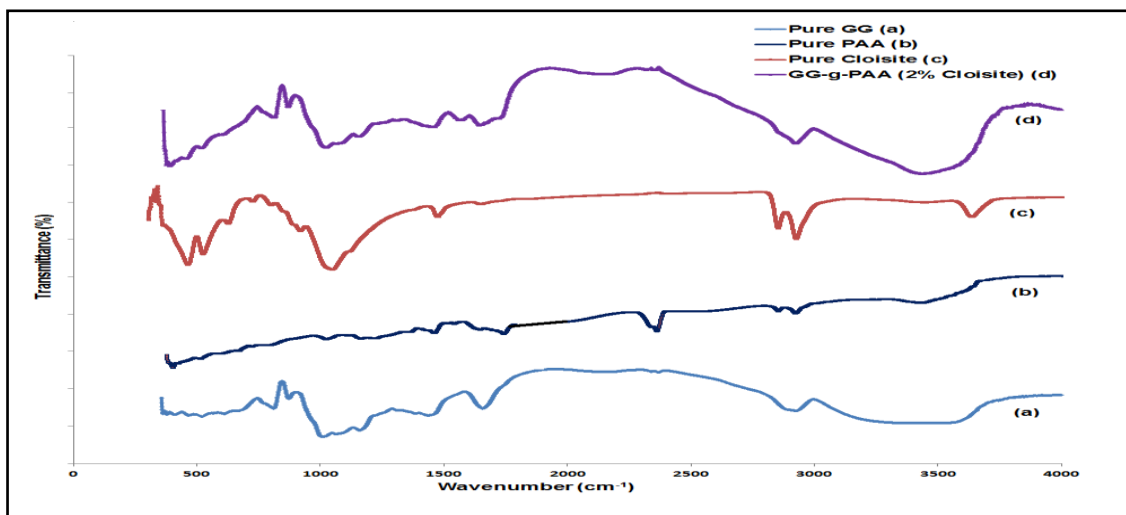


Figure 1: FTIR spectrum of (a) Pure GG, (b) Pure PAA, (c) Pure cloisite and (d) GG-g-PAA/2% cloisite.

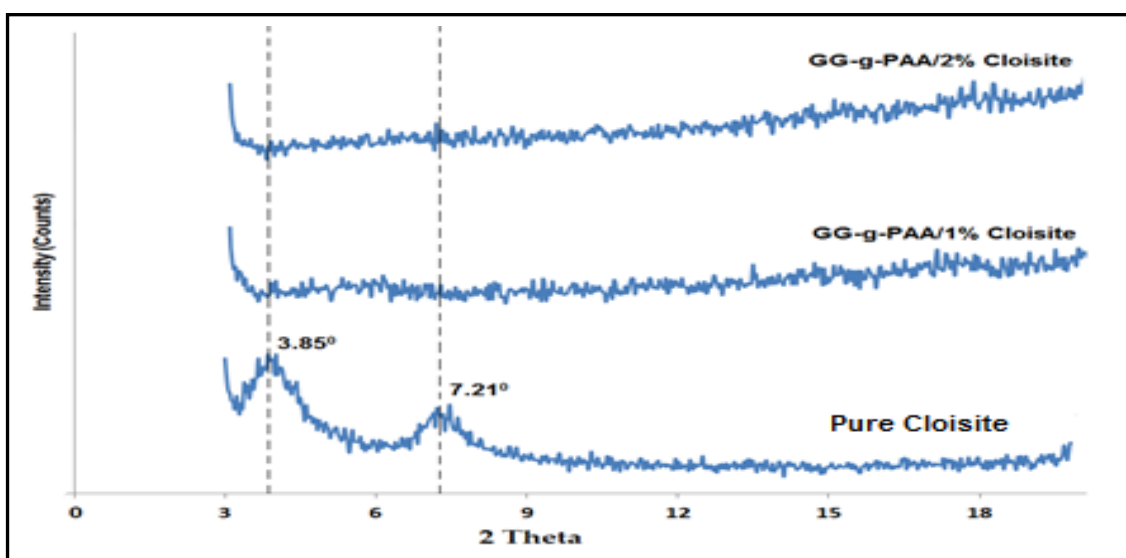


Figure 2: XRD of pure cloisite, grafted guar gum with 1% cloisite and 2% cloisite.

the soil. At regular intervals, they were removed, rinsed properly, dried completely and weighed. The loss of weight was calculated as given below in Eq (4). Weight loss,

$$WL = \frac{W_b - W_a}{W_b} * 100 \quad (4)$$

Where, W_b and W_a are the weights of the dried sample before and after being buried in the soil respectively

3. RESULTS AND DISCUSSION

3.1. FTIR analysis

The FTIR spectra of (a) pure guar gum, (b) pure PAA (c) pure cloisite and (d) GG-g-PAA/2% cloisite have been shown in the Fig1. It can be observed that guar gum (Fig. 1a) shows the

characteristic absorption peaks at 1027 and 1148 cm^{-1} ascribed to bending of $\text{CH}_2\text{-O-CH}_2$ and the band at 3406 cm^{-1} is ascribed to the bending vibration of -O-H stretching [12].

The FTIR spectrum of PAA (Fig. 1b) has a prominent band at 1752 cm^{-1} associated with COO stretching. In addition, there are peaks at 2860 and 2936 cm^{-1} which can be assigned to CH , CH_2 stretching. The characteristic absorption peaks of cloisite are located at 2932, 2855 and 1467 cm^{-1} in the FTIR spectrum of pure cloisite as in Fig.1(c), which were assigned to C-H vibrations of methylene groups (asymmetric stretching, symmetric stretching and bending respectively) [13]. However, after graft-copolymerization with PAA the FTIR spectrum of GG-g-PAA nanocomposites with 2% cloisite (Fig 1d) shows a

weakened absorption band at 1017 and 1170 cm^{-1} which is attributable to bending of $\text{CH}_2\text{-O-CH}_2$, whereas, these peaks were quite strong for pure guar gum as depicted in Fig 1(a). Further, the characteristic peaks at 1752 cm^{-1} of PAA and at 2850-2950 cm^{-1} of PAA and cloisite have been disappeared from the FTIR spectrum of GG-g-PAA/2% cloisite. This indicates PAA and cloisite have been grafted onto guar gum backbone

3.2. XRD analysis

XRD analysis was performed to assess the clay dispersion within the polymer matrix. The XRD patterns of GG-g-PAA nanocomposites with 1% and 2% Cloisite have been shown in Fig 2. The figure also includes the XRD patterns of pure cloisite for the sake of comparison. Fig.2 clearly shows that the lower crystalline peaks at $2\theta=3.85^\circ$ and $2\theta=7.21^\circ$ that are present in the pure cloisite have disappeared from XRD pattern of GG-g-PAA/cloisite nanocomposites. This clearly indicates the exfoliation of cloisite in guar gum [14-15].

3.3 Comparison of conventional and microwave grafting

The time of reaction has been optimized to give highest graft percentage. Table 1(a) and 1(b) shows comparison of conventional and microwave grafting technique with respect to time. In conventional synthesis, the optimum reaction time was 60 mins with 60.61% grafting (Table 1(a)) and in microwave it was just 4.5 mins with 63.64% grafting (Table 1(b)). Increased reaction times, reduces the graft percentage owing to active site reduction and inevitable homo-polymer formation (Tables 1(a) and (b)). Thus, the microwave technique is much faster as compared to the conventional method [16].

3.4 Effect of cloisite concentration on swelling

A series of GG-g-PAA/cloisite nanocomposites were prepared by varying the concentration of cloisite from 0 to 5% (w/w). Equilibrated swelling (ES) calculated has been plotted against cloisite content as shown in Fig 3. From the figure, it can be observed that the highest ES has been obtained at 2% (w/w) cloisite concentration. Further increase in cloisite concentration decreases ES. The incorporation of rigid nanoclay prevents intertwining of grafted polymeric chains and weakens the hydrogen bonding interaction between -COOH groups. This decreases the degree of physical cross linking and improves water absorption [17]. When the concentration of nanoclay increases they may act as additional crosslinking points in polymer networks and thus increases cross linking density which reduces the network voids for holding water. Moreover they

Table 1 (a). Grafting percentage of reaction in Conventional method at varying time.

Time (mins)	Grafting (%)
45	6.06
48	15.15
51	21.21
54	36.36
57	36.36
60	60.61

Table 1 (b). Grafting percentage of reaction in Microwave method at varying time.

Time (mins)	Grafting (%)
2	3.03
2.5	12.12
3	21.21
3.5	27.27
4	42.42
4.5	63.64

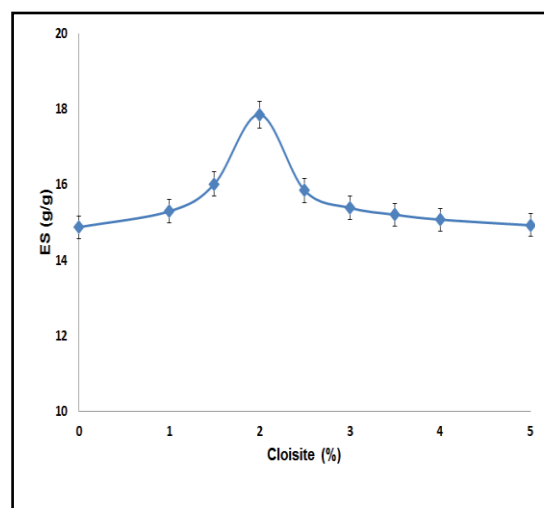


Figure 3: Effect of cloisite concentration on water absorbency.

may also fill the voids, decreasing the hydrophobicity of the nanocomposite. Similar reports on the improvement of water absorbency have been observed [1]. Addition of 5% montmorillonite (MMT) showed an improvement of water absorbency due to the presence of active -OH groups on MMT surface.

3.5 Effect of various buffers on swelling

The study of swelling behavior in acidic, basic and neutral buffer medium is shown in the Fig 4. Acidic medium shows better swelling than in basic and neutral medium. The ES value in acidic medium (curve a) increases over time and reaches a maximum of 22.24 g/g in 120 minutes. Beyond 2 hrs the ES drops and is then stabilized i.e., equilibrium is attained. This trend is generally called an over-shooting effect, where the ES shoots up initially and then lowers before attaining various

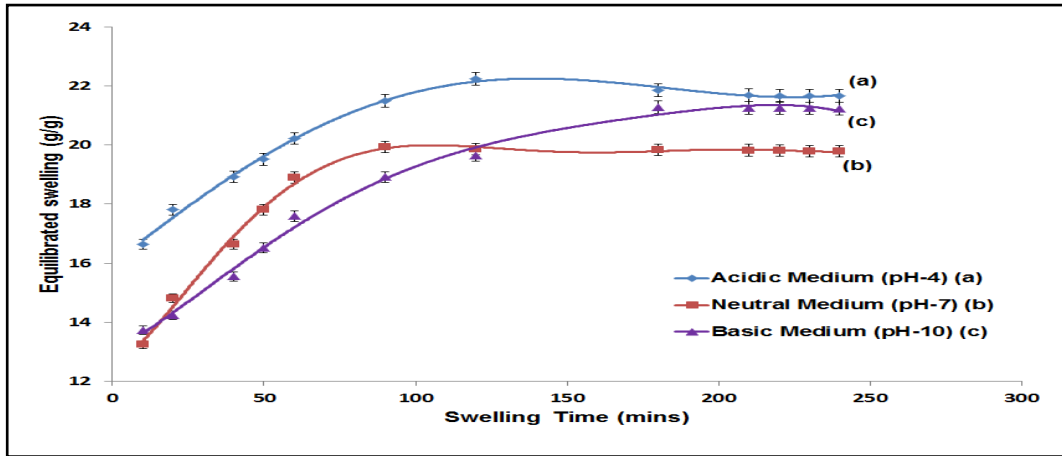


Figure 4: Swelling studies in various buffer medium.

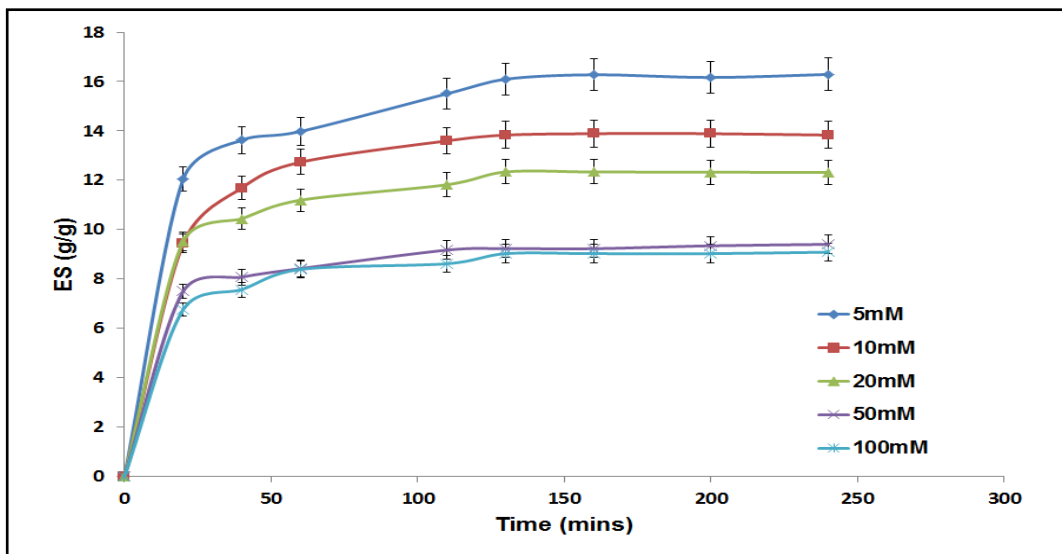


Figure 5: Effect of NaCl concentration on swelling of GG-g-PAA/2% Cloisite.

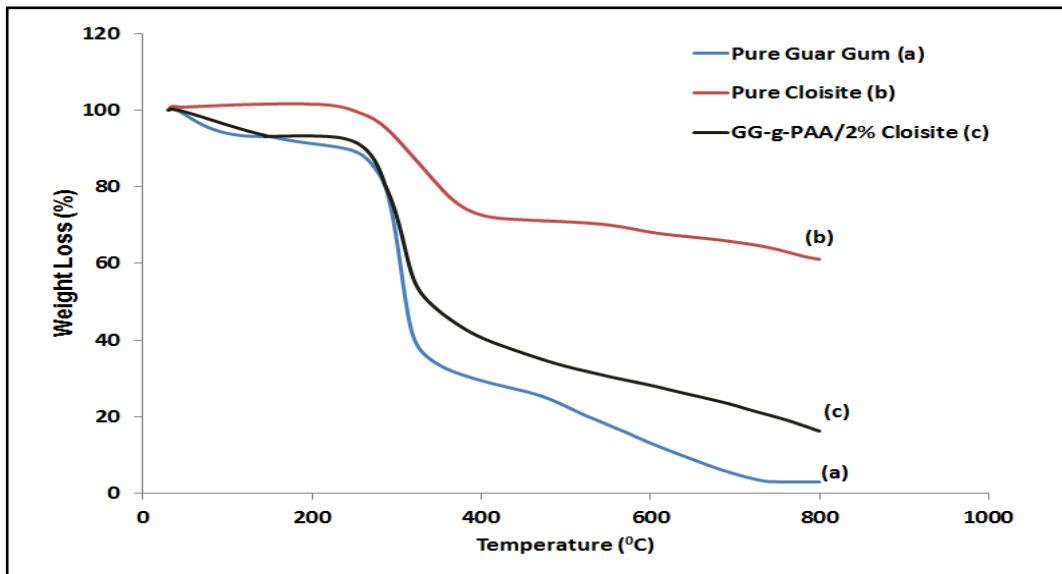


Figure 6: TGA curves of (a) Pure GG, (b) Pure Cloisite and (c) GG-g-PAA/2% Cloisite.

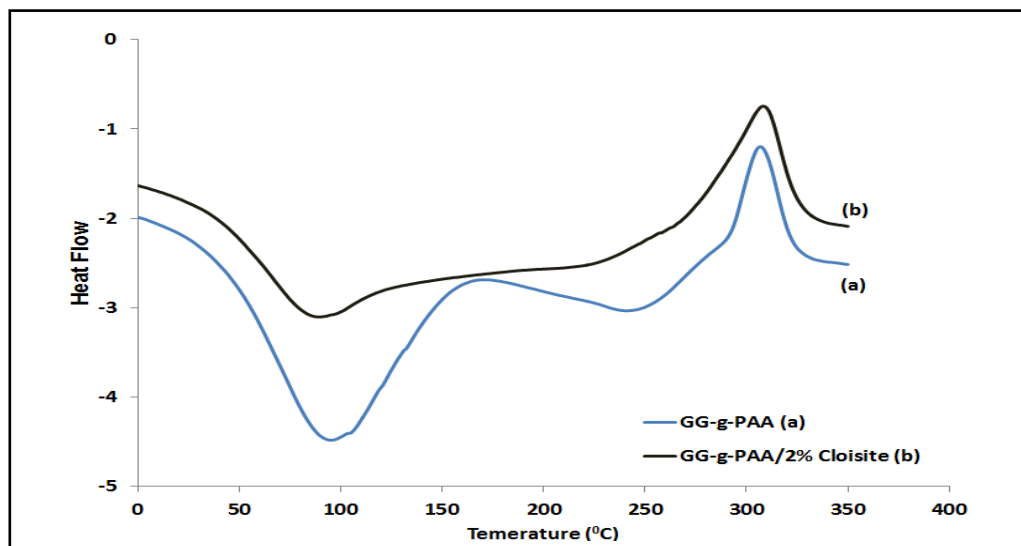


Figure 7: DSC curves of (a) GG-g-PAA and (b) GG-g-PAA/2% Cloisite.

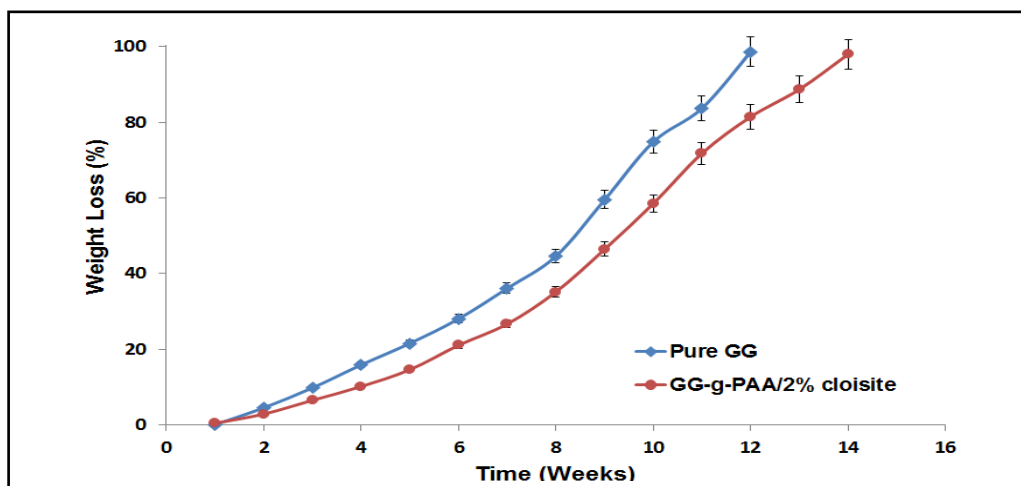


Figure 8: Biodegradation characteristics of (a) Pure GG and (b) GG-g-PAA/2% Cloisite.

equilibrium. But in this figure the effect is rather not very significant. However, significant observations have been made by researchers on many types of composites. Most of the researchers attribute this trend to co-operative physical cross-linking, which is a process where chemical cross-linking and physical cross-linking are cooperative [18]. When such crosslinking occurs it reduces the amount of water being retained in the polymer, hence the reduction in ES. The over-shoot effect decreases with increase in pH. This is visible from curve (b) and curve (c) which represent the swelling behavior of the composite in neutral and basic medium, respectively.

3.6 Effect of saline concentration on swelling

Fig 5 shows the effect of NaCl concentration on swelling of GG-g-PAA/Cloisite. The ES is generally less than that in distilled water. This can be attributed to the change in osmotic pressure in the environment. The same reason results in the

decrease in the swelling as the concentration of the salt is increased. At low NaCl concentration the swelling rate of the composite is faster than at higher concentrations. The factors that caused the water absorption in the polymer included the osmotic pressure difference between the interior and the exterior of the polymer. The increasing osmotic pressure with increase of salt concentration led to the decrease in osmotic pressure difference between the interior and exterior of the superabsorbent polymer. Similar observations were made by Li et.al [19] on wheat straw graft polymers. The way a hydrogel behaves in ionic solutions affects its applicability in retaining physiological fluids and in pharmaceutical applications.

3.7 TGA analysis

Fig 6 shows the thermograms of pure GG, pure cloisite and GG-g-PAA/Cloisite nanocomposites. From the figure it can be observed that the onset of

thermal degradation for pure GG (curve a) occurs at 238°C with a weight loss of 10%. On the other hand, GG-g-PAA/Cloisite nanocomposites (curve c) have a weight loss of 8% at 238°C. This indicates that thermal stability of nanocomposites increased with the addition of cloisite. Cloisite being a ceramic material will usually have better thermal stability [13]. Addition of cloisite provides a transient protective barrier to both mass and energy transport in nanocomposites [20-21]. Hence, incorporation of Cloisite improves the thermal stability of the nanocomposites

3.8 DSC analysis

The DSC thermograms of GG-g-PAA and GG-g-PAA/2% cloisite are given in Fig 7. It can be observed that, GG-g-PAA composites show two endothermic peaks at 94°C and 241°C and one exothermic peak at 304°C. Even, GG-g-PAA/2% cloisite nanocomposites show two endothermic peaks at 94°C and 227°C and one exothermic peak at 307°C. The initial peak at 94°C corresponds to oxidation of water contents. It is also observed that the addition of cloisite reduces the peak temperature of endothermic peak. This shift suggests that there is a reduction in crystalline size and crystal imperfection due to improved compatibility between guar gum and the nanoclay as suggested by Liu et. al [14]. Compared to the sharp curve of GG-g-PAA, the peak of GG-g-PAA/Cloisite becomes broader. A similar observation made by Wang et.al [22] on CMC-g-poly(sodiumacrylate)/stone superabsorbent composites suggests that the widening of peaks depicts the delay of thermal decomposition of the SAP after the addition of the nanoclay. However, on the other hand, it is observed that the addition of cloisite increases the peak temperature of endothermic peak. This can be attributed to the increase in oxidation temperature of the nanocomposites.

3.9. Biodegradation studies

Fig 8(a) and (b) shows the biodegradation plot of percentage weight loss versus time for pure GG and GG-g-PAA/2% cloisite nanocomposites, respectively. A time lag before the onset of degradation can be observed in both the curves. This is owing to the time taken by the soil microorganisms to adapt to the new components. It can be observed that the percentage biodegradability of the nanocomposites stays lesser than that of the natural polysaccharide. This can be attributed to the natural enhancement in the interactions within the molecule owing to graft modification and incorporation of the nanomaterial which restricts the segmental motion at the interface causing the effective path length and diffusion time to increase. A similar observation

has been made by Rimdusit et.al [23] for methylcellulose–montmorillonite (MMT) composites.

4. CONCLUSION

In this study, guar gum-grafted-Poly acrylic acid/cloisite superabsorbent nanocomposites have been synthesized by grafting poly (acrylic acid) onto the backbone guar gum. Organically modified nanoclay (cloisite) has been incorporated in order to enhance the properties of the superabsorbent polymer. Comparison of conventional and microwave methods showed that the microwave technique can considerably reduce the amount of time required to complete the reaction by 98% and able to obtain better grafting percentage. Characterization using FTIR and XRD indicates efficient grafting of PAA onto the GG backbone and the exfoliation of cloisite in guar gum, respectively. The swelling studies showed that, optimal swelling equilibrium of nanocomposites have been achieved at 2% cloisite loading. The incorporation of Cloisite clearly improved the thermal stability of the superabsorbent. Biodegradation studies revealed that the percentage biodegradability of the nanocomposites stays lesser than that of the natural polysaccharide. However, complete degradation has been achieved within 15 weeks. Thus, due to its water retention properties and biodegradable nature, this nanocomposite can be used as eco-friendly superabsorbents.

Acknowledgements

The authors would like to thank the Department of Science and Technology (DST) for financial support of this work under the green chemistry program.

5. REFERENCES

- [1]. W. Wang, J. Zhang and A. Wang, (2009) Preparation and swelling properties of superabsorbent nanocomposites based on natural guar gum and organo-vermiculite, *Applied Clay Science*, **46**: 21-26.
- [2]. F. Puoci, F. Iemma, U.G. Spizzirri, G. Cirillo, M. Curcio and N. Picci, (2008) Polymer in agriculture: A review, *American Journal of Agricultural and Biological Sciences*, **3**: 299–314.
- [3]. K. Kosemund, H. Schlatter, J.L. Ochsenhirt, E.L. Krause, D.S. Marsman and G.N. Erasala, (2009) Safety evaluation of superabsorbent baby diapers, *Regulatory Toxicology and Pharmacology*, **53**: 81–89.
- [4]. L. Wang, J.P. Zhang and A.Q. Wang, (2008) Removal of methylene blue from aqueous solution using chitosan-g-poly (acrylic acid)/montmorillonite superadsorbent

- nanocomposite, *Colloid Surface A*, **322**: 47–53.
- [5]. M. Sadeghi and H.J. Hosseinzadeh, J. Bioact, (2008) Synthesis of starch-poly(sodium acrylate-co-acrylamide) superabsorbent hydrogel with salt and pH-responsiveness properties as a drug delivery system, *Journal of Bioactive and Compatible Polymers*, **23**: 381–404.
- [6]. A. Pourjavadi, S. Barzegar and G.R. Mahdavinia, (2006) MBA-crosslinked Na-Alg/ CMC as a smart full-polysaccharide superabsorbent hydrogels, *Carbohydrate Polymers*, **66**: 386–395.
- [7]. S. Siva Prasad, K. Madhusudhana Rao, P. Rama Subba Reddy, N. Sivagangi Reddy, K.S.V. Krishna Rao, M.C.S. Subha, Synthesis and Characterisation of Guar Gum-g-Poly(Acrylamidoglycolic acid) by Redox Initiator, *Indian Journal of Advances in Chemical Science* 1(1) (2012) 28-32.
- [8]. P. Liu, (2007) Polymer modified clay minerals: A review, *Applied Clay Science*, **38**: 64-76.
- [9]. H.M. Park, X. Li, C.Z. Jin, C.Y. Park, W.J. Cho and C.K. Ha, (2002) Preparation and properties of biodegradable thermoplastic starch/clay hybrids, *Macromolecular Materials and Engineering*, **287**: 553–558.
- [10]. X.J. Huang, S.M. Xu, M. Zhong, J.D. Wang, S. Feng and R.F. Shi, (2009) Modification of Na-Bentonite by polycations for fabrication of amphoteric semi-IPN nanocomposite hydrogels, *Applied Clay Science*, **42**: 455-459.
- [11]. W. Wang and A. Wang, (2009) Preparation and properties of superabsorbent nanocomposites based on natural guar gum and modified rectorite, *Applied Clay Science*, **77**: 891-897.
- [12]. G. Dodi, D. Hritcu and M.I. Popa, (2011) Carboxymethylation of guar gum: Synthesis and Characterization, *Cellulose Chemistry and Technology*, **45**: 171-176.
- [13]. A.T. Petroula, (2011) Composites of Engineering Plastics with Layered Silicate Nanofillers: Preparation and Study of Microstructure and Thermomechanical Properties. *Nanocomposites and Polymers with analytical method*, **978**: 307-352.
- [14]. P.S. Liu, L. Li, N.L. Zhou, J. Zhang, S.H. Wei and J. Shen, (2007) Waste Polystyrene Foam-graft-acrylic acid/Montmorillonite Superabsorbent Nanocomposite, *Journal of Applied Polymer Science*, **104**: 2341-2349.
- [15]. W. Luo, W. Zhang, P. Chen and Y. Fang, (2005) Synthesis and properties of starch grafted poly(acrylamide-co-acrylic acid)/montmorillonite nanosuperabsorbent via γ -ray irradiation technique, *Journal of Applied Polymer Science*, **96**: 1341-1346.
- [16]. Z.Y. Peng and F.G. Chen, (2010) Synthesis and Properties of Temperature-Sensitive Hydrogel Based on Hydroxyethyl Cellulose, *International Journal of Polymeric Materials*. **59**: 450-461.
- [17]. E. Al, G. Guclu, T.B. Iyim, S. Emik and S. Ozgumus, (2010) Removal of Cu^{2+} and Pb^{2+} ions from aqueous solutions by starch-graft-acrylic acid/montmorillonite superabsorbent nanocomposite hydrogels, *Polymer Bulletin*, **65**: 333-346.
- [18]. Y. Yin, X. Ji, H. Dong, Y. Ying and H. Zheng, (2008) Study of the swelling dynamics with overshooting effect of hydrogels based on sodium alginate-g-acrylic acid, *Carbohydrate Polymers*, **71**: 682-689.
- [19]. W.F. Lee, and R.J. Wu, (1996) Superabsorbent Polymeric Materials. I. Swelling Behaviors of Crosslinked Poly(sodium acrylate-co-hydroxyethyl methacrylate) in Aqueous Salt Solution. *Journal of Applied Polymer Science*, **62**: 1099-1114.
- [20]. A.P.P. Soto, S.S. Valdes and L.F.R. Devalle, Macromol. (2007) Morphological and Thermal Properties of ABS/Montmorillonite Nanocomposites Using ABS with Different AN Contents, *Macromolecular Materials and Engineering*, **292**: 302-309.
- [21]. H.S. Kim, B.H. Park, J.H. Choi and J.S. Yoon, (2008) Preparation and Mechanical Properties of Acrylonitrile-Butadiene-Styrene Copolymer/Clay Nanocomposites. *Journal of Applied Polymer Science*, **107**: 2539-2544.
- [22]. W. Wang, Q. Wang and A. Wang, (2011) pH-responsive carboxymethyl cellulose-g-poly(sodium acrylate)/polyvinyl pyrrolidone semi-IPN hydrogels with enhanced responsive and swelling properties, *Macromolecular Research*, **19**: 57-65.
- [23]. S. Rimdusit, S. Jingjid, S. Damrongsakkul, S. Tiptikaporn and T. Takeichi, (2008) Biodegradability and property characterizations of Methyl Cellulose: Effect of nanocompositing and chemical crosslinking, *Carbohydrate Polymers*, **72**: 444-455.